Journal of Physics and Chemistry of Solids 151 (2021) 109909

Contents lists available at ScienceDirect

Journal of Physics and Chemistry of Solids

journal homepage: http://www.elsevier.com/locate/jpcs

Technical note

Enhanced self-healing of irradiation defects near a Ni–graphene interface by damaged graphene: Insights from atomistic modeling

Hai Huang [a,b,*], Xiaobin Tang [b,**], Kun Xie [a], Qing Peng [c]

[a] Key Laboratory of Materials Physics of Ministry of Education, School of Physics and Microelectronics, Zhengzhou University, Zhengzhou, 450052, China
[b] Department of Nuclear Science & Technology, Nanjing University of Aeronautics and Astronautics, Nanjing, 210016, China
[c] Physics Department, King Fahd University of Petroleum & Minerals, Dhahran, 31261, Saudi Arabia

ARTICLE INFO

Keywords:
Nickel–graphene interface
Enhanced self-healing
Irradiation-induced defects
Damaged graphene
Atomistic simulations

ABSTRACT

Graphene-reinforced nickel matrix nanocomposites with high-density interfaces are recommended as candidate materials for advanced nuclear reactors because of the potential irradiation tolerance. Nonetheless, the mechanism that graphene damage due to irradiation affects the tolerance of the composites remains unclear. Here we report the relationships between irradiation damage behavior of graphene and defect sink efficiency of nickel–graphene interface by using atomistic simulations. With the accumulation of irradiation dose, a nickel–graphene interface exhibits enhanced trapping ability to defects despite the gradually deteriorative damage of graphene. The enhancement originates in that the damaged regions of graphene can provide abundant recombination and/or annihilation sites for irradiation defects and strengthen the energetic and kinetic driving forces of the interface to defects. This study reveals a new possible interface-mediated damage healing mechanism of irradiated materials.

Ni–graphene nanocomposites (NGNC) have been proven to have excellent mechanical properties, high thermal/electrical conductivity, and enhanced corrosion resistance, and recently attracted tremendous attention in the automobile, aerospace, and nuclear industries [1–5]. More importantly, with plenty of ultra-high-strength Ni–graphene interfaces (NGIs), the composites may also have excellent irradiation tolerance. Many researches have demonstrated that grain boundaries (GBs) and phase interfaces can attract, absorb, and annihilate point and line defects produced in materials subjected to extreme radiation [6–13]. Analogically, NGIs will probably improve the self-healing ability of irradiation defects for the composites. Consequently, the applications of NGNC may be further extended to the structural materials for nuclear reactors where high irradiation tolerance is a primary concern. For instance, in Gen-IV nuclear reactors, one of the primary candidate materials, Ni-based alloys, will be exposed to the higher temperatures and higher neutron doses than those of current-generation reactors, causing the acceleration of irradiation degradation of the materials [14–18]. Due to the significant superiority, NGNC may provide a pathway for resolving the dilemma of Ni-based alloys.

To explore the feasibility of the above idea, several studies about irradiation simulations and experiments of NGNC have been carried out. On the modeling and simulation side, it has been clearly shown that NGIs can act as effective sinks for irradiation-induced defects, such as interstitials, vacancies, and He atoms/clusters, and retard the nucleation and growth of defect clusters [19–21]. Experimentally, NGNC exhibits lesser crystal defects (*e.g.*, lattice swelling and stacking faults) and smaller He bubbles than those in pure Ni under energetic ion irradiation [22]. These studies have preliminarily demonstrated NGNC with excellent irradiation tolerance. However, a worrying issue has emerged but rarely received attention by far. The intrinsically ordered lattice arrangement of graphene (Gr) in NGNC would transform into a disordered structure with high-density topological defects due to irradiation [23–26]. In consideration of the importance of Gr in forming NGIs, the structural disorder of Gr may dramatically affect the trapping ability of NGIs and even pose a huge challenge to the potential of NGNC in irradiation-tolerant materials. Therefore, understanding the inherent relationships between irradiation damage behavior of Gr and sink efficiency of NGI is of fundamental importance to develop NGNC with resisting irradiation failure.

In this work, the issue was addressed from two aspects. On one hand,

* Corresponding author. Key Laboratory of Materials Physics of Ministry of Education, School of Physics and Microelectronics, Zhengzhou University, Zhengzhou, 450052, China.
** Corresponding author.
E-mail addresses: huanghai@zzu.edu.cn (H. Huang), tangxiaobin@nuaa.edu.cn (X. Tang).

https://doi.org/10.1016/j.jpcs.2020.109909
Received 5 September 2020; Received in revised form 27 October 2020; Accepted 15 December 2020
Available online 17 December 2020

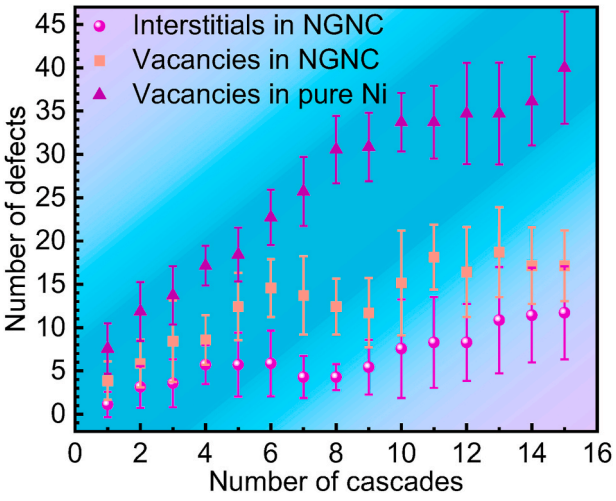

Fig. 1. The number of surviving point defects in the bulk of NGNC versus the number of cascades. The number of vacancies in pure Ni is also shown for comparison.

molecular dynamics (MD) was adopted to simulate cascade overlaps near the NGIs. We aim at investigating the effects of NGIs on the accumulation of surviving defect production in their Ni bulk as the irradiation damage of Gr aggravates. On the other hand, the formation energies, binding energies, and diffusion barriers of Ni defects near the NGIs with differently irradiation-damaged Gr were calculated by molecular statics (MS). The purpose is to reveal what changes have happened about the energetic and kinetic driving forces of damaged NGIs to Ni defects relative to those of pristine NGIs to Ni defects.

All simulations were carried out using the parallel MD code LAMMPS [27], and visualizations were rendered with OVITO [28]. The sandwich NGI models constructed in our previous work [19] were also adopted. The interactions between Ni atoms, the interactions among C atoms in Gr, and the Ni–C interactions were described by the embedded atom method (EAM) potential [29], the adaptive intermolecular reactive empirical bond order (AIREBO) potential [30], and the Lennard–Jones potential [31], respectively. The setting of each potential, the creation and optimization of NGI model, and the identification of interface and bulk regions have been described elsewhere [19,21].

By performing MD simulations, we accumulated up to 15 single cascades in the same cell at the temperature of 300 K, one after the other (detailed in Supplementary Material). Each primary knock-on atom (PKA) with 5.0 keV was initialized at a distance of 15.0 Å away from the Gr plane and perpendicularly directed toward the NGI, eventually inducing cascade overlaps (see Fig. S1). Wigner–Seitz cell method [19, 32] was used to identify the point defects (*i.e.*, Ni interstitials and vacancies) in the bulk. The number of point defects surviving in the bulk versus the number of cascades is shown in Fig. 1, in which each data point is a mean of 10 independent runs. The number of vacancies in pure Ni is also displayed for comparison. Clearly, the number of interstitials in the bulk is always less than that of vacancies after each cascade, implying that NGIs prefer to trap interstitials and leave a higher concentration of vacancies behind in the bulk. The number of defects in pure Ni is often more than that of NGNC, and the difference between the two gradually widens with the increasing number of cascades, suggesting that NGIs can continuously facilitate the recombination and annihilation of the point defects produced during cascade overlaps. Due to this effect, the point defects in the bulk can be eliminated or dispersed as far as possible, eventually making defect clusters difficult to form in NGNC than in pure Ni after the consecutive PKA bombardment (see Fig. S2). Furthermore, the number of defects in pure Ni presents a significant (or approximately linear) increase with the increasing number of cascades. Generally, within 20 overlapped cascades, the trend is very common for traditional nuclear materials [33–36] and even novel nanocrystalline alloys (*e.g.* Ni [37] and Zr [38], in which the sink character of GBs has not substantially enhanced or degenerated after cascade overlaps). However, the number of surviving defects in the bulk only exhibits a slightly escalating trend with the increasing number of cascades. After the tenth overlapped cascades, the escalating trend is further abated, and especially, the number of vacancies fluctuates very little, exhibiting a different trend compared to those mentioned above. In other words, with the accumulation of irradiation dose, the self-healing of irradiation defects can be further enhanced by the NGI, while almost no change for other structural materials.

Fig. 2 shows the surface morphologies of Gr within the NGI captured after the first, fourth, eighth, twelfth, fourteenth, and fifteenth overlapped cascades, respectively. It can be seen that with the increasing number of cascades, the area of irradiation damage of Gr gradually increases, and all small damage regions of Gr tend to aggregate into a single large damage region since the C chains jointing the different

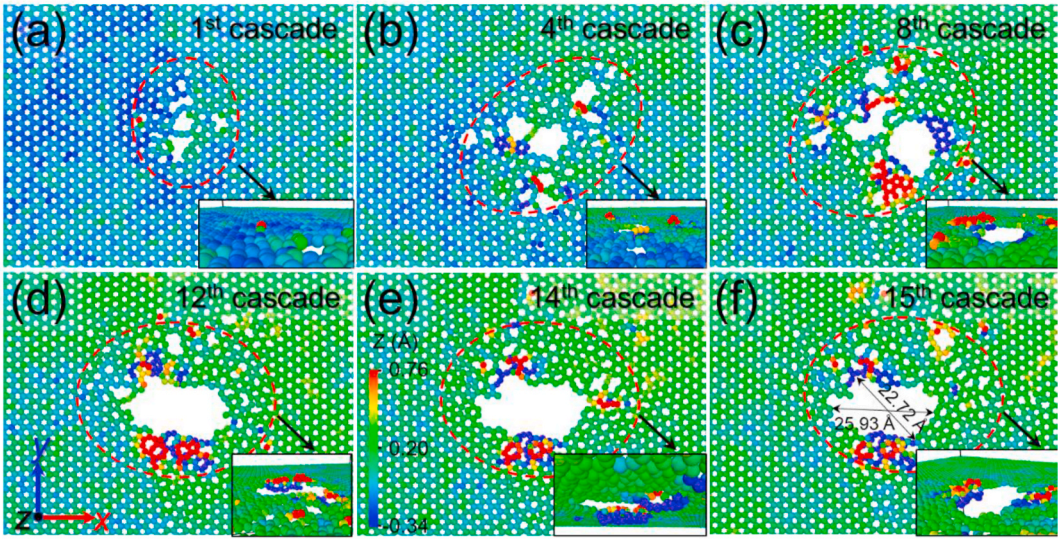

Fig. 2. Snapshots of the Gr of NGNC captured after the first (**a**), fourth (**b**), eighth (**c**), twelfth (**d**), fourteenth (**e**), and fifteenth (**f**) overlapped cascades. C atoms are colored according to their z-coordinates centering on the Gr plane. The damaged region of Gr is singled out with a red oval and enlarged in the insets. Each panel is on the same scale bar.

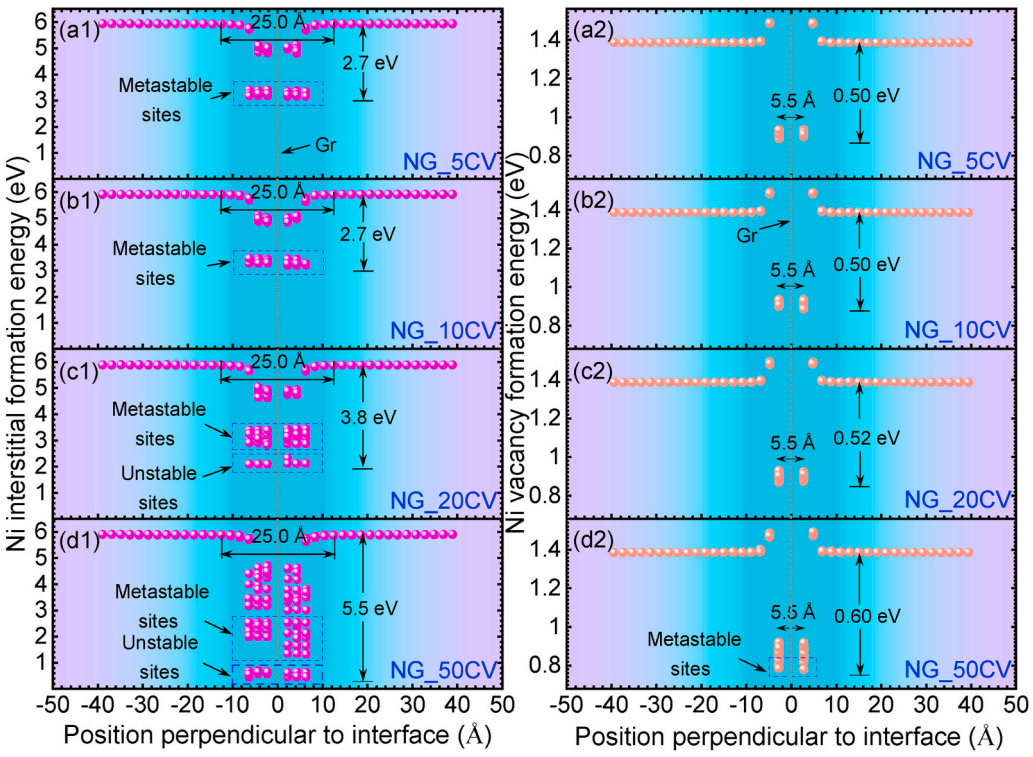

Fig. 3. Interstitial and vacancy formation energies of Ni near the C-vacancy modified NGI of NG_5CV ((**a1**) and (**a2**)), NG_10CV ((**b1**) and (**b2**)), NG_20CV ((**c1**) and (**c2**)), or NG_50CV ((**d1**) and (**d2**)) as a function of the initial distance of the defect from the corresponding Gr plane. The defect segregation energy and interaction zone of each NGI to the defect are also exhibited. The metastable and unstable sites are marked by blue dotted boxes.

damage regions also gradually break. After the fifteenth overlapped cascades, the size of Gr damage region exceeds 20 Å. Meanwhile, the displacement degrees of C atoms along the z-axis are also intensified accordingly, further deteriorating the intrinsic order of Gr. The excessively displaced carbon atoms are not escaped from the Gr to enter the deep bulk region but absorbed on the Gr surface discretely, which further aggravates the disordering of the Gr after each cascade. These suggest that there is a roughly positive response relationship between the damage degree of Gr and the number of cascades. Besides, after cascade overlaps, Ni defects within the NGI will also accumulate gradually because of the trapping effect of NGI [19]. As a consequence, the special defect structure, with C and Ni defects simultaneously localized at the NGI, may strongly modify the NGI and thus, affect further evolution of irradiation defects near the NGI. And the more disordered the NGI, the more prominent the effect may be. As mentioned in our previous work [19], the sink strength of NGIs can be further enhanced by the loaded Ni defects, which exhibits a noticeable difference from that of GBs [39] and may be one of the reasons for the above phenomenon about the enhanced self-healing of irradiation defects. Analogically, it can be speculated that the damaged Gr due to irradiation may be also responsible for the change of the sink character of NGI.

To provide a more intuitive understanding to the effect of above damaged Gr on the sink character of NGI, four smaller NGNC systems that capture the salient features of differently damaged Gr due to overlapped cascades, were designed and used to calculate the energetics and kinetics of irradiation-induced defects within a certain range of the NGIs. Further details of the model building and calculations are provided within the Supplemental Material and our previous work [19]. The four systems, modified by 5, 10, 20, and 50 C vacancies on their corresponding Gr (see Fig. S3), are defined as NG_5CV, NG_10CV, NG_20CV, and NG_50CV, respectively. The interstitial and vacancy formation energies of Ni as a function of distance for the four damaged NGIs are exhibited in Fig. 3. A striking feature is that the defect formation energy tends to decrease as the defect approach each NGI, indicating that there are still attractive interactions between Ni defects and C-vacancy modified NGIs. Compared with the calculations of pristine NGIs [19], the interaction length ranges of C-vacancy modified NGIs to Ni defects almost have no change, while the defect formation energies further decline within the damaged NGIs. The extent of the decline of interstitial formation energy is more obvious than that of vacancy formation energy. Especially, the interstitial formation energy within the NGI of NG_50CV further decreases by approximately 5.0 eV relative to that of pristine NGIs. In the vicinity of the four damaged NGIs, the vacancy segregation energies are 0.50, 0.50, 0.52, and 0.60 eV, while the interstitial segregation energies are 2.7, 2.7, 3.8, and 5.5 eV, respectively, all of which are higher than those of pristine NGIs. This implies significantly increasing attraction to Ni defects from C-vacancy modified NGIs relative to pristine NGIs. Besides, the defect segregation energy presents an increasing trend with the increase of the number of C vacancies, suggesting that the sink strengths of NGIs are gradually enhanced with the increase of Gr damage. However, the segregation strengths of the four damaged NGIs to vacancies are lower than those of Ni-interstitial modified NGIs (with 10 interstitials) to vacancies, while the segregation strengths of C-vacancy modified NGIs to interstitials tend to be consistent with those of Ni-interstitial modified NGIs (with 10 interstitials) to interstitials when the number of C vacancies reaches 50 [19], implying that C-vacancy modified NGIs have weaker sink strengths than those of Ni-interstitials modified NGIs.

Another noticeable feature can also be observed from Fig. 3. The trend of defect formation energy near the C-vacancy modified NGIs almost has no change when the number of C vacancies is less than 20. However, as the number of C vacancies exceeds 20 and further increases, the defect formation energy shows a gradually sinking trend within the damaged NGIs, and its value range is also further widened. The reason may be that there are only some metastable sites for Ni defects near the damaged NGIs when the number of C vacancies is less than 20, while as the number of C vacancies exceeds 20, more and more unstable sites for Ni defects also begin to appear due to the formation of C defect clusters

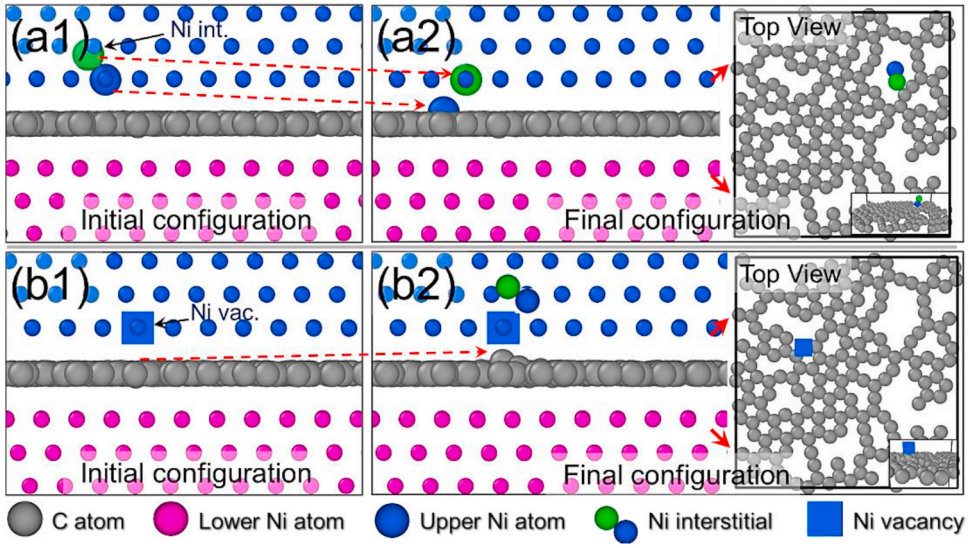

Fig. 4. Configurations of the NG_50CV with single Ni interstitial ((**a1**) and (**a2**)) or vacancy ((**b1**) and (**b2**)) near the NGI before and after static relaxation.

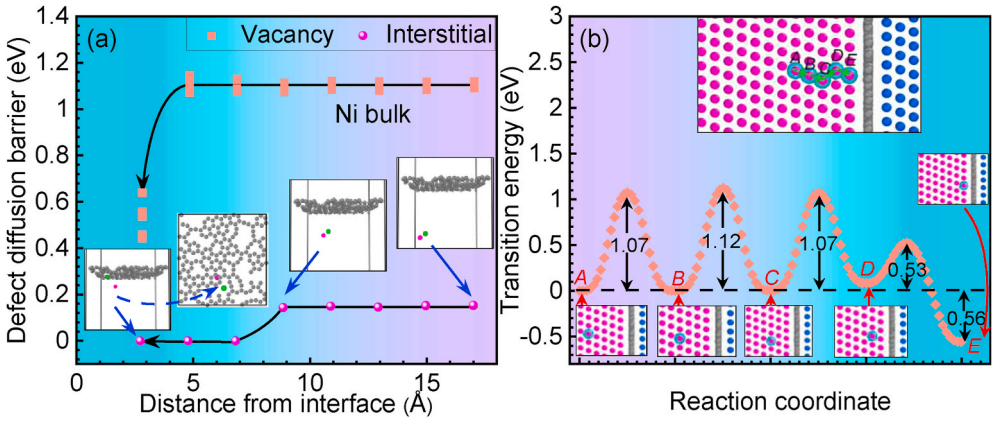

Fig. 5. Defect diffusion near the NGI of NG_50CV. (**a**) Vacancy and interstitial diffusion barriers as a function of distance from the C-vacancy modified NGI. (**b**) One diffusion–annihilation path for a vacancy. The system energy at position A is selected as the reference energy.

(see Fig. S3). The emergence of metastable states means that there is a tendency of recombination and/or annihilation between Ni defects and Gr damage, while the unstable sites form spontaneously trapping and/or annihilation regions around the C defect clusters loaded at the NGIs. To clarify the speculation vividly, the initial NG_50CV model with single Ni interstitial or vacancy near the NGI is statically relaxed and then exhibited in Fig. 4. Only this system was considered because the recombination and/or annihilation events are more likely to occur near its NGI relative to those of the other three systems. After relaxation, the Ni interstitial quickly slides into a C defect cluster on the Gr, and the Ni vacancy tends to attract the dangling C atoms at the edge of Gr damage, all of which trigger recombination and/or annihilation and then result in the further decrease of system energy. From this, it can be determined that the C vacancies and C defect clusters on the Gr should be the source of the aforementioned metastable and unstable sites of Ni defects, respectively, which make the segregation strengths of NGIs to Ni defects enhance.

Next, the defect diffusion barriers toward the NGIs in different migration paths were calculated using the climbing-image nudged elastic band (CI-NEB) method [40]. The configurations that are fully relaxed for calculating defect formation energies in Fig. 3 were used as the initial and final states. The kinetic details of the optimum migration paths and diffusion barriers have been described elsewhere [19]. Only the diffusion barrier of Ni defect within a certain range of the NGI of NG_CV50 is shown in Fig. 5(a), the reason for which is similar to that of static relaxation in Fig. 4. Clearly, the vacancy and interstitial diffusion barriers in the bulk of NG_50CV do not show significant fluctuations like as those near the Ni-interstitial modified NGIs, while is very consistent with those near the pristine NGIs [19], which may be since the Gr damage does not cause obvious lattice distortion and stress environment of Ni bulk (see Fig. 4). However, the vacancy diffusion barrier close to the damaged NGI shows a certain degree of decline relative to that of pristine NGIs (the maximum decline approximately 0.2 eV). The events that interstitials spontaneously enter NGIs and are trapped by NGIs, are more likely to occur near the damaged NGI than near the pristine NGIs, because the interstitial diffusion barrier is reduced to zero faster. The reason for these phenomena may be consistent with the large fluctuations in the formation energies within the damaged NGIs in Fig. 3. Also, one diffusion–annihilation path is exhibited in Fig. 5(b) to monitor the evolution of the system energy as a vacancy approaches the damaged NGI. It can be seen that the vacancy, before entering the interface, must break through a barrier of 0.53 eV that is reduced by 0.15 eV compared with that of pristine NGIs [19]. Meanwhile, when the vacancy stays in the NGI, the system energy reduces by 0.56 eV that is further 0.1 eV less than that of pristine NGIs [19]. These suggest that Ni defects more easily migrate into C-vacancy modified NGIs than pristine NGIs, eventually causing the system to release more energy.

In summary, using classical MD simulations, we have found that with

the accumulation of irradiation dose, the sink character of a NGI still works well. Peculiarly, although the damage degree of Gr within the NGI gradually aggravates, the self-healing of irradiation defects in the bulk is further enhanced by the NGI instead. The MS calculations indicated that damaged Gr needs to be responsible for the enhancement of sink efficiency of NGI since the damaged regions of Gr easily form metastable and unstable sites of Ni defects and facilitate the occurrence of deep recombination and/or annihilation of Ni defects. On the other hand, the energetic and kinetic driving forces of NGIs to Ni defects become stronger and stronger with the deteriorative irradiation damage of Gr. As a consequence, NGNC exhibits a unique character: the higher the irradiation dose, the more excellent the irradiation tolerance. Note that the character may be only feasible under the premise that the stability of NGIs still can be maintained by damaged Gr [21,41]. All these results reveal an unconventional mode for the self-healing of irradiation defects near the NGIs and motivate further understanding of irradiation tolerance of NGNC applied in advanced nuclear energy systems.

CRediT authorship contribution statement

Hai Huang: Conceptualization, Methodology, Software, Writing - original draft, Visualization, Supervision, Funding acquisition. **Xiaobin Tang:** Conceptualization, Validation, Writing - review & editing, Supervision. **Kun Xie:** Visualization, Writing - review & editing. **Qing Peng:** Validation, Investigation, Writing - review & editing.

Declaration of competing interest

The authors declare that they have no known competing financial interests or personal relationships that could have appeared to influence the work reported in this paper.

Acknowledgments

This work was supported by the National Natural Science Foundation of China (Grant No. 11705087) and the Henan Supercomputing Center.

Appendix A. Supplementary data

Supplementary data to this article can be found online at https://doi.org/10.1016/j.jpcs.2020.109909.

References

[1] Y. Kim, J. Lee, M.S. Yeom, J.W. Shin, H. Kim, Y. Cui, J.W. Kysar, J. Hone, Y. Jung, S. Jeon, S.M. Han, Strengthening effect of single-atomic-layer graphene in metal–graphene nanolayered composites, Nat. Commun. 4 (2013) 1–7.
[2] D. Kuang, L. Xu, L. Liu, W. Hu, Y. Wu, Graphene–nickel composites, Appl. Surf. Sci. 273 (2013) 484–490.
[3] Y. Lei, J. Jiang, T. Bi, J. Du, X. Pang, Tribological behavior of in situ fabricated graphene–nickel matrix composites, RSC Adv. 8 (2018) 22113–22121.
[4] L. Ji, F. Chen, H. Huang, X. Sun, Y. Yan, X. Tang, Preparation of nickel–graphene composites by jet electrodeposition and the influence of graphene oxide concentration on the morphologies and properties, Surf. Coating. Technol. 351 (2018) 212–219.
[5] Z. Chen, P. Wei, S. Zhang, B. Lu, L. Zhang, X. Yang, K. Huang, Y. Huang, X. Li, Q. Zhao, Graphene reinforced nickel-based superalloy composites fabricated by additive manufacturing, Mat. Sci. Eng. A 769 (2020) 138484.
[6] C.M. Parish, K. Wang, P.D. Edmondson, Nanoscale chemistry and crystallography are both the obstacle and pathway to advanced radiation-tolerant materials, Scripta Mater. 143 (2018) 169–175.
[7] G. Meric de Bellefon, I.M. Robertson, T.R. Allen, J.C. van Duysen, K. Sridharan, Radiation-resistant nanotwinned austenitic stainless steel, Scripta Mater. 159 (2019) 123–127.
[8] R. Gao, M. Jin, F. Han, B. Wang, X. Wang, Q. Fang, Y. Dong, C. Sun, L. Shao, M. Li, J. Li, Superconducting Cu/Nb nanolaminate by coded accumulative roll bonding and its helium damage characteristic, Acta Mater. 197 (2020) 212–223.
[9] N. Gao, D. Perez, G. Lu, Z. Wang, Molecular dynamics study of the interaction between nanoscale interstitial dislocation loops and grain boundaries in BCC iron, J. Nucl. Mater. 498 (2018) 378–386.
[10] X. Li, Y. Zhang, Y. Xu, X. Wu, X. Kong, X. Wang, Q. Fang, C. Liu, Interaction of radiation-induced defects with tungsten grain boundaries at across scales: a short review, Tungsten 2 (2020) 15–33.
[11] X. Zhang, K. Hattar, Y. Chen, L. Shao, J. Li, C. Sun, K. Yu, N. Li, M.L. Taheri, H. Wang, J. Wang, M. Nastasi, Radiation damage in nanostructured materials, Prog. Mater. Sci. 96 (2018) 217–321.
[12] Y. Kim, J. Baek, S. Kim, S. Kim, S. Ryu, S. Jeon, S.M. Han, Radiation resistant vanadium-graphene nanolayered composite, Sci. Rep. 6 (2016) 1–9.
[13] Y. Liu, Y. Zeng, Q. Guo, J. Zhang, Z. Li, D. Xiong, X. Li, D. Zhang, Bulk nanolaminated graphene (reduced graphene oxide)-aluminum composite tolerant of radiation damage, Acta Mater. 196 (2020) 17–29.
[14] M.A. Stopher, The effects of neutron radiation on nickel-based alloys, Mater. Sci. Technol. 33 (2017) 518–536.
[15] Z. Zhu, H. Huang, J. Liu, J. Gao, Z. Zhu, Xenon ion irradiation induced hardening in inconel 617 containing experiment and numerical calculation, J. Nucl. Mater. 525 (2019) 32–39.
[16] A.F. Rowcliffe, L.K. Mansur, D.T. Hoelzer, R. K, Perspectives on radiation effects in nickel-base alloys for applications in advanced reactors, J. Nucl. Mater. 392 (2009) 341–352.
[17] H.G. MacPherson, The molten salt reactor adventure, Nucl. Sci. Eng. 90 (1985) 374–380.
[18] Q. Peng, F. Meng, Y. Yang, C. Lu, H. Deng, L. Wang, S. De, F. Gao, Shockwave generates< 100> dislocation loops in bcc iron, Nat. Commun. 9 (2018) 1–6.
[19] H. Huang, X. Tang, F. Chen, F. Gao, Q. Peng, L. Ji, X. Sun, Self-healing mechanism of irradiation defects in nickel–graphene nanocomposite: an energetic and kinetic perspective, J. Alloys Compd. 765 (2018) 253–263.
[20] G. Ge, F. Chen, X. Tang, H. Huang, X. Sun, L. Ji, Phase-field modeling of helium bubble evolution in nickel-graphene nanocomposite, J. Appl. Phys. 125 (2019) 215304.
[21] H. Huang, X. Tang, F. Gao, F. Chen, G. Ge, Y. Yan, Q. Peng, Release of helium-related clusters through a nickel–graphene interface: an atomistic study, Appl. Surf. Sci. 487 (2019) 218–227.
[22] H. Huang, X. Tang, F. Chen, J. Liu, X. Sun, L. Ji, Radiation tolerance of nickel–graphene nanocomposite with disordered graphene, J. Nucl. Mater. 510 (2018) 1–9.
[23] K.P. So, D. Chen, A. Kushima, M. Li, S. Kim, Y. Yang, Z. Wang, J.G. Park, Y.H. Lee, R.I. Gonzalez, M. Kiwi, E.M. Bringa, L. Shao, J. Li, Dispersion of carbon nanotubes in aluminum improves radiation resistance, Nano Energy 22 (2016) 319–327.
[24] W. Yao, L. Fan, The effect of ion irradiation induced defects on mechanical properties of graphene/copper layered nanocomposites, Metals 9 (2019) 733.
[25] W.J. Huang, W.Y. Woon, Ion implantation of graphene with keV carbon ions: defect types, evolution and substrate effects, Vacuum 166 (2019) 72–78.
[26] Z. Bai, L. Zhang, H. Li, L. Liu, Nanopore creation in graphene by ion beam irradiation: geometry, quality, and efficiency, ACS Appl. Mater. Interfaces 8 (2016) 24803–24809.
[27] S. Plimpton, Fast parallel algorithms for short-range molecular dynamics, J. Comput. Phys. 117 (1995) 1–19.
[28] A. Stukowski, Visualization and analysis of atomistic simulation data with OVITO–the Open Visualization Tool, Model. Simulat. Mater. Sci. Eng. 18 (2009), 015012.
[29] G. Bonny, N. Castin, D. Terentyev, Interatomic potential for studying ageing under irradiation in stainless steels: the FeNiCr model alloy, Model. Simulat. Mater. Sci. Eng. 21 (2013), 085004.
[30] S.J. Stuart, A.B. Tutein, J.A. Harrison, A reactive potential for hydrocarbons with intermolecular interactions, J. Chem. Phys. 112 (2000) 6472–6486.
[31] S.P. Huang, D.S. Mainardi, P.B. Balbuena, Structure and dynamics of graphite-supported bimetallic nanoclusters, Surf. Sci. 545 (2003) 163–179.
[32] A. Hosseini, M.N. Nasrabadi, A. Esfandiarpour, Effect of carbon nanotube on radiation resistance of CNT-Cu nanocomposite: MD simulation, J. Mater. Sci. 55 (2020) 4311–4320.
[33] F. Gao, W.J. Weber, Cascade overlap and amorphization in defect accumulation, topological features, and disordering, Phys. Rev. B 66 (2002), 024106.
[34] K. Vörtler, N. Juslin, G. Bonny, L. Malerba, K. Nordlund, The effect of prolonged irradiation on defect production and ordering in Fe–Cr and Fe–Ni alloys, J. Phys-Condens. Mat. 23 (2011) 355007.
[35] Y. Dai, L. Ao, Q. Sun, L. Yang, J. Nie, S. Peng, X. Long, X. Zhou, X. Zu, L. Liu, X. Sun, D. Terentyev, F. Gao, Nucleation of Cr precipitates in Fe–Cr alloy under irradiation, Comput. Mater. Sci. 101 (2015) 293–300.
[36] G. Martin, C. Sabathier, J. Wiktor, S. Maillard, Molecular dynamics study of the bulk temperature effect on primary radiation damage in uranium dioxide, Nucl. Instrum. Methods B 352 (2015) 135–139.
[37] A. Arjhangmehr, S.A.H. Feghhi, A. Esfandiyarpour, F. Hatami, An energetic and kinetic investigation of the role of different atomic grain boundaries in healing radiation damage in nickel, J. Mater. Sci. 51 (2016) 1017–1031.
[38] F. Hatami, S.A.H. Feghhi, A. Arjhangmehr, A. Esfandiarpour, Interaction of primary cascades with different atomic grain boundaries in α-Zr: an atomic scale study, J. Nucl. Mater. 480 (2016) 362–373.
[39] X. Li, W. Liu, Y. Xu, C. Liu, B. Pan, Y. Liang, Q. Fang, J. Chen, G. Luo, Z. Wang, Y. Dai, Self-blocking of Interstitial Clusters Near Metallic Grain Boundaries, vol. 1505, 2015, 07202 arXiv preprint.
[40] G. Henkelman, B.P. Uberuaga, H. Jónsson, A climbing image nudged elastic band method for finding saddle points and minimum energy paths, J. Chem. Phys. 113 (2000) 9901–9904.
[41] L. He, S. Si, H. Xu, C. Tang, J. Liu, S. Dong, C. Jiang, X. Xiao, Enhanced mechanical property and radiation resistance of reduced grapheneoxide/tungsten composite with nacre-like architecture, Compos. Struct. 245 (2020) 112361.